SUPPLEMENTARY VIEW FIGURE LEGENDS

Figure S1. TFG forms octameric ring-like structures. (a) Schematic representation of human and *C. elegans* TFG isoforms. The PB1 (Phox and Bem1p) domain, the coiled-coil motif (CC), and the proline- and glutamine-rich (PQ rich) region are highlighted in each protein. Boundaries of each domain are highlighted by amino acid number. (b) Negative stain images of full-length *C. elegans* TFG (top left), truncated *C. elegans* TFG (top right, amino acids 1-195), full-length human TFG (bottom left), and truncated human TFG (bottom right, amino acids 1- 193). Scale bar, 30 nm. (c) Coomassie stained SDS-PAGE gels of purified *C. elegans* and human TFG that were used for EM analysis (truncated isoforms on the left and full-length isoforms on the right).

Figure S2. Domain organization and architecture of the TFG amino-terminus. (a) Sequence alignment of the amino-terminal domains of human and *C. elegans* TFG isoforms. The PB1 domains are highlighted in green, and the coiled-coil motifs are indicated in red. Asterisks show amino acids that are conserved between the two species. (b) Cryo image of truncated *C. elegans* TFG (amino acids 1-195). Scale bar, 30 nm. (c) Recombinant, full length *C. elegans* TFG particle size was determined using dynamic light scattering following the addition of various salts. Error bars represent mean +/- SEM; 10 replicates.

Figure S3. The carboxyl-terminus of TFG is highly enriched with disordering amino acids. (a) The sequence of human TFG was analyzed by DISOPRED2 to reveal regions predicted to adopt a helical conformation (pink), a β-sheet conformation (yellow), or exhibit intrinsic disorder (red boxes). (b) The sequence of *C. elegans* TFG was analyzed similarly as described for panel

a. (c) *C. elegans* TFG was subjected to limited proteolysis (using 4 nM chymotrypsin) in the presence or absence of potassium acetate (300 mM) for various amounts of time. At each timepoint indicated, samples were boiled in the presence of SDS, resolved by SDS-PAGE, and stained using Coomassie.

Figure S4. Organization of the early secretory pathway in human cells. (a) Mammalian BSC-40 cells were transiently transfected with a plasmid encoding mCherry-Sec61β and stained with either Sec16A antibodies (left) or ERGIC-53 antibodies (right). Cells were imaged using structured illumination microscopy and images shown are projections of 3D data sets (2 μm in z). Merged images with mCherry-Sec61β in red and either Sec16A (left) or ERGIC-53 (right) in green are shown (at least 15 cells were analyzed for each condition). Scale bar, 1 μm. (b) Human RPE-1 cells stably expressing low levels of mApple-Sec16B were fixed and stained using antibodies directed against endogenous Sec16A. Cells were imaged using SR-SIM and images shown are projections of 3D data sets (2 μm in z). Both individual and merged images with Sec16A in green and mApple-Sec16B in red are shown (at least 8 individual cells were analyzed). Scale bar, 2 μm. (c) Human RPE-1 cells were fixed and stained using antibodies directed against endogenous Sec16A and TFG. Cells were imaged using SR-SIM and images shown are projections of 3D data sets (4 μm in z). Both individual and merged images with Sec16 in green and TFG in red are shown (representative of more than 10 cells that were analyzed). Scale bar, 5 μm. Higher magnification views of the indicated regions (boxed) are also shown in the upper right portion of each image. Inset scale bar, 1 μm. (d) Human RPE-1 cells were fixed and stained using antibodies directed against endogenous Sec16A and ERGIC-53. Cells were imaged using structured illumination microscopy and images shown are

projections of 3D data sets (4 μm in z). Both individual and merged images with Sec16 in green and ERGIC-53 in red are shown (representative of more than 10 cells that were analyzed). Scale bar, 5 μm. Higher magnification views of the indicated regions (boxed) are also shown in the upper right portion of each image. Inset scale bar, 1 μm. (e) Human RPE-1 cells were fixed and stained using antibodies directed against the endogenous forms of Sec16A, TFG, and ERGIC-53. Cells were imaged using confocal microscopy and images shown are projections of 3D data sets (4 μm in z). Both individual and merged images with ERGIC-53 in blue, TFG in green, and Sec16A in red are shown (n=15). Scale bar, 5 μm. Higher magnification views of the indicated regions (boxed) are also shown in the upper right portion of each image. Inset scale bar, 1 μm. (f and g) Human RPE-1 cells were fixed and stained using antibodies directed against the endogenous forms of TFG and ERGIC-53. Cells were imaged using SR-SIM (f) or confocal microscopy (g) and images shown are projections of 3D data sets (4 μm in z). Both individual and merged images with ERGIC-53 in green and TFG in red are shown (more than 10 cells were analyzed for each condition). Scale bar, 5 μm. Higher magnification views of the indicated regions (boxed) are also shown in the upper right portion of each image. Inset scale bar, 1 μm. TFG exhibits a distinct distribution as compared to ERGIC-53. (h) Human RPE-1 cells were fixed and stained using antibodies directed against the endogenous forms of TFG and GM130. Cells were imaged using confocal microscopy and images shown are projections of 3D data sets (4 μm in z). Both individual and merged images with TFG in green and GM130 in red are shown (representative of more than 10 cells that were analyzed). Scale bar, 5 μm. Higher magnification views of the indicated regions (boxed) are also shown in the upper right portion of each image. Inset scale bar, 2 μm. TFG exhibits a distinct distribution as compared to GM130, even within the region of the perinuclear Golgi ribbon.

Figure S5. Both the amino- and carboxyl-terminal portions of TFG are important for its distribution in cells. (a) GST and GST-tagged full-length human TFG were co-expressed with a polyhistidine-tagged, truncated form of TFG (amino acids 1-193) and immobilized on glutathione agarose beads. Following an extensive series of washes, proteins were eluted using reduced glutathione, separated by SDS-PAGE, and stained using Coomassie. Purified GST-tagged full-length TFG is shown on the left for comparison. The amino-terminal fragment of TFG specifically co-purifies with GST-tagged full-length TFG, but not GST alone. (b and c) Human RPE-1 cells transiently transfected with plasmids encoding either GFP fused to amino acids 1-350 (b) or amino acids 1-300 (c) of TFG were fixed and stained using antibodies directed against endogenous Sec31A and TFG. Cells were imaged using confocal microscopy and images shown are projections of 3D data sets (4 μm in z). Both individual and merged images with GFP-TFG (residues 1-350 or 1-300) in green, Sec31A in red, and TFG in blue are shown (more than 15 cells were analyzed for each condition). Scale bar, 5 μm. Higher magnification views of the indicated regions (boxed) are also shown. Inset scale bar, 1 μm. (d and e) Human RPE-1 cells depleted of endogenous TFG were transiently transfected with plasmids overexpressing either amino acids 1-350 (d) or amino acids 1-300 (e) of TFG, fixed and stained using antibodies directed against endogenous Sec31A and TFG. Cells were imaged using confocal microscopy and images shown are projections of 3D data sets (4 μm in z). Both individual and merged images with truncated TFG in green and Sec31A in red are shown (more than 10 cells were analyzed for each condition). Scale bar, 5 μm. Higher magnification views of the indicated regions (boxed) are also shown. Inset scale bar, 1 μm.

Figure S6. Depletion of TFG leads to apoptosis and the loss of COPII-coated transport carrier clustering. (a) Control cells (mock treated), cells depleted of TFG using siRNAs targeting the 3'UTR or coding exon 1 (72 hours post-transfection), and cells treated with a low concentration of tunicamycin (10 μg/mL for 72 hours) were harvested, lysed, and extracts were separated by SDS-PAGE, followed by Coomassie staining or immunoblotting for TFG, Sec23A, Caspase 3, and α-tubulin (loading control). Caspase 3 cleavage (an indicator of apoptotic initiation) is observed following 72 hours of TFG siRNA treatment or long-term incubation with low concentrations of tunicamycin. A serial dilution of the control extract was loaded to quantify depletion levels. (b) Cells were grown for 24, 60, or 72 hours after TFG siRNA treatment and incubated with NucView 488, a caspase 3 substrate, which accumulates bright fluorescence in the nucleus of cells undergoing apoptosis. During the later timecourse of siRNA treatment, cells become highly elongated and fail to continue to proliferate (with a mitotic index of 0.25%, which was significantly lower than control cells that exhibited a mitotic index of 3.6%; n=400 cells for each condition; $p<0.01$ calculated using a paired *t* test), as observed in DIC images. (c) Cells were counted in at least 10 distinct imaging fields at 24, 48, 60, and 72 hours after siRNA treatment. Error bars represent mean +/- SEM; experiments were performed on at least 3 separate occasions for each time point. (d) Human RPE-1 cells were fixed and stained using antibodies directed against the endogenous forms of ERp57 (an ER marker) and Sec31A. Cells were imaged using confocal microscopy, and images shown are projections of 3D data sets (1 μm in z). Merged images with ERp57 in green and Sec31A in red are shown (representative of more than 15 cells that were analyzed). Scale bar, 1 μm. (e) Graph showing the average percentage of GFP-tagged Sec23A fluorescence recovered as a function of time in seconds relative to the bleach in control and TFG depleted cells (error bars represent means +/- SEM for

each time; n=15 different cells for each condition). Only puncta that remained in a single imaging plane throughout the time lapse acquisition were included in the analysis. (f) The distribution of endogenous Sec31A was examined using immunogold-EM in control and TFG depleted cells using 10 nm gold particles bound to α-Sec31A antibodies. For these experiments, grids were stained with 2% uranyl acetate in methanol for 1 minute. Additionally, freeze substitution was completed in 12 hours, and cells were subsequently rinsed three times in acetone and put directly into 100% Lowicryl HM20. Small arrowheads highlight putative COPII transport carriers that are clustered in control cells. At least 5 different cells were analyzed for each condition, and representative images are shown. Scale bar, 100 nm.

Figure S7. Overexpression of TFG induces the formation of aberrant, enlarged foci that titrate inner and outer COPII components and transport carriers. (a) Human RPE-1 cells were transiently transfected with a plasmid encoding GFP-TFG, then fixed and stained using TFG antibodies and imaged using confocal microscopy. Images shown are individual confocal sections, illustrating that the TFG antibody fails to penetrate the enlarged foci. By contrast, GFP-TFG is observed throughout the aberrant structures. Both individual and merged images with GFP-TFG in green and total TFG in red are shown (representative of more than 20 cells analyzed). Scale bar, 5 μm. Higher magnification views of the indicated regions (boxed) are also shown in the lower left portion of each image. Inset scale bar, 1 μm. (b) Human RPE-1 cells were transiently transfected with a plasmid encoding untagged TFG, fixed and stained using Sec31A and TFG antibodies and imaged using confocal microscopy. Images shown are individual confocal sections. Both individual and merged images with TFG in green and Sec31A in red are shown (representative of more than 20 cells that were analyzed). Scale bar, 5

μm. Higher magnification views of the indicated regions (boxed) are also shown in the upper right portion of each image. Inset scale bar, 1 μm. (c) Quantification of the number of Sec31A-labeled structures in a 4 μm^2 region in cells depleted of endogenous TFG and ectopically expressing either untagged TFG or GFP-tagged TFG. For both conditions, at least 20 distinct regions away from the perinuclear Golgi were examined. Error bars represent mean +/- SEM; at least 5 different cells per condition. **$p < 0.05$ compared with control, calculated using a paired *t* test. (d) Negative stain images of untagged (left) or amino-terminally hemagglutinin (HA) tagged human TFG (amino acids 1-193). Scale bar, 30 nm. (e) Human RPE-1 cells that inducibly overexpress TFG were incubated in the presence or absence of 1 μg/mL doxycycline for 48 hours and lysed in sample buffer. Extracts were separated by SDS-PAGE and immunoblotted using TFG or β-actin antibodies. (f) Human RPE-1 cells that inducibly overexpress TFG were incubated in the presence or absence of 1 μg/mL doxycycline for 24 hours. Cells were subsequently fixed and stained using antibodies directed against endogenous Sec31A and TFG. Cells were imaged using confocal microscopy and images shown are projections of 3D data sets (4 μm in z). Merged images with TFG in green and Sec31A in red are shown (representative of more than 15 cells that were analyzed). Inducible expression of TFG is coupled to the expression of soluble mApple (pseudo-colored blue). Scale bar, 5 μm. (g) The distribution of endogenous TFG was examined using immunogold-EM in TFG overexpressing cells using 15 nm gold particles bound to α-TFG antibodies. For these experiments, grids were stained with 2% uranyl acetate in methanol for 1 minute followed by 3 seconds of lead citrate. Small arrowheads highlight membranous transport carriers associate with enlarged TFG foci. At least 12 different cells were analyzed, and representative images are shown. Scale bars, 100 nm.

Figure S8. Overexpression of TFG induces the formation of aberrant, enlarged foci that associate with Sec16-enriched ER membranes and titrate COPII transport carriers. (a) Human RPE-1 cells stably expressing low levels of mRuby-Sec23A were transiently transfected with a plasmid encoding untagged TFG, then fixed and stained using TFG antibodies and imaged using confocal microscopy. Images shown are projections of 3D data sets (4 μm in z). Both individual and merged images with TFG in green and Sec23A in red are shown (n=19 cells). Scale bar, 5 μm. (b) Mammalian BSC-40 cells were transiently transfected with plasmids encoding untagged TFG and mCherry-Sec61β, then fixed and stained using Sec31A antibodies and imaged using confocal microscopy. Images shown are individual confocal sections. Both individual and merged images with Sec31A in green and Sec61β in red are shown (representative of more than 10 cells that were analyzed). Scale bar, 5 μm. Higher magnification views of the indicated regions (boxed) are also shown in the upper left portion of each image. Inset scale bar, 1 μm. (c) Human RPE-1 cells stably expressing low levels of mApple-Sec16B were transiently transfected with a plasmid encoding untagged TFG, fixed and stained using TFG antibodies and imaged using confocal microscopy. Images shown are individual confocal sections. Both individual and merged images with TFG in green and mApple-Sec16B in red are shown (n=12 cells). Scale bar, 5 μm.

Figure S9. Overexpression of TFG disrupts early secretory pathway organization. (a) The distribution of endogenous ERGIC-53 was examined in cells transiently transfected with a plasmid encoding untagged TFG (n=15 cells). Scale bar, 5 μm. Inset scale bar, 1 μm. (b) Human RPE-1 cells stably expressing low levels of mannosidase II-mApple (ManII) (top row) or

mApple-Sec16B (bottom row) were fixed and stained using β-COP antibodies and imaged using confocal microscopy (top panels). Images shown are projections of 3D data sets (4 μm in z). Both individual and merged images with β-COP in green and ManII or Sec16B in red are shown (at least 15 cells were analyzed for each condition). Scale bar, 5 μm. Higher magnification views of the indicated regions (boxed) are also shown in the lower portion of each image. Inset scale bar, 2 μm. (c) Human RPE-1 cells were transiently transfected with a plasmid encoding untagged TFG, then fixed and stained using β-COP and TFG antibodies and imaged using confocal microscopy (n=15). Images shown are projections of 3D data sets (4 μm in z). Merged images with β-COP in green and TFG in red are shown. Scale bar, 5 μm. Higher magnification views of the indicated regions (boxed) are also shown in the lower right portion of each image. Inset scale bar, 2 μm. Note that the methanol fixation procedure necessary to observe β-COP staining results in a morphological change (crenation) in the enlarged TFG foci. (d) Human RPE-1 cells were transiently transfected with a plasmid encoding untagged TFG, then fixed and stained using GM130 and TFG antibodies and imaged using confocal microscopy. Images shown are projections of 3D data sets (4 μm in z). Merged images with TFG in green and GM130 in red are shown (n=10 cells). Scale bar, 10 μm. (e) Higher magnification views of the indicated regions (boxed areas 1 and 2 in panel d) are shown. Scale bar, 5 μm. (f) Human RPE-1 cells were transiently transfected with plasmids encoding GFP-SQSTM1, fixed and stained using Sec31A antibodies and imaged using confocal microscopy. Images shown are projections of 3D data sets (4 μm in z). Both individual and merged images with GFP-SQSTM1 in green and Sec31A in red are shown (n=10 cells). Scale bar, 5 μm. Higher magnification views of the indicated regions (boxed) are also shown in the lower portion of each image. Inset scale bar, 1 μm. (g) Human RPE-1 cells that were either mock depleted or depleted of TRAPPC3 were fixed

and stained using GM130 antibodies and imaged using confocal microscopy (n=15 cells). Images shown are projections of 3D data sets (6 μm in z). Scale bar, 5 μm. (h) Human RPE-1 cells that were either mock depleted or depleted of TRAPPC3 were fixed and stained using Sec16A and Sec31A antibodies and imaged using confocal microscopy (n=15 cells). Images shown are projections of 3D data sets (6 μm in z). Cells treated with TRAPPC3 siRNA consistently become elongated during the course of the treatment. Merged images with Sec16A in green and Sec31A in red are shown. Scale bar, 5 μm. (i) Higher magnification views of the boxed regions (shown in panel h) are shown. Scale bar, 1 μm.

SUPPLEMENTARY MOVIE LEGENDS

Movie S1. TFG octamers undergo reversible polymerization. Purified *C. elegans* full-length TFG was labeled directly with BODIPY-FL and added to a hanging drop of buffer containing 100 mM KOAc on a glass coverslip. Upon addition of 300 mM KOAc, TFG structures assemble on the surface of the glass. However, upon addition of water to dilute the salt, the TFG structures rapidly disassemble.

Movie S2. Depletion of TFG increases the number of COPII-labeled transport carriers. Cells stably expressing low levels of GFP-tagged Sec23A were imaged using swept-field confocal microscopy (500 msec intervals between acquisitions). COPII-labeled transport carriers exhibit similar dynamics when comparing control cells (left) and TFG depleted cells (right), although their numbers vary significant between conditions.

Movie S3. Depletion of TFG does not significantly affect the recovery of GFP-Sec23A fluorescence after photobleaching. Cells stably expressing low levels of GFP-tagged Sec23A were imaged using swept-field confocal microscopy (500 msec intervals between acquisitions). Approximately 5 seconds after the initiation of time-lapse imaging, a region of the cell was photobleached, and then normal image acquisition resumed. The kinetics of GFP-tagged Sec23A fluorescence recovery was similar in the presence (left) or absence (right) of TFG.

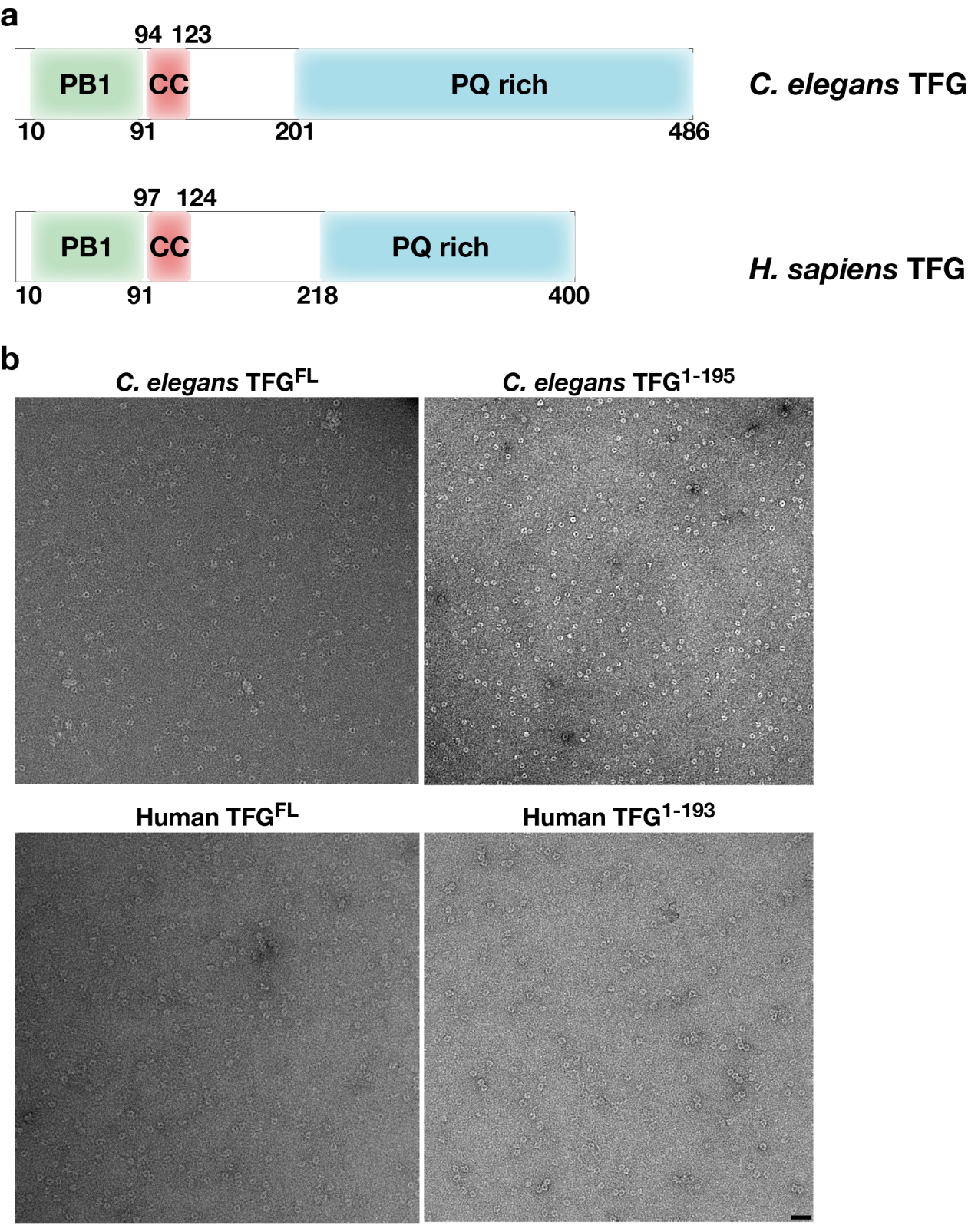
a
94 123
PB1
CC
PQ rich
10
91
201
486
C. elegans TFG
97 124
PB1
CC
PQ rich
10
91
218
400
H. sapiens TFG
b
C. elegans TFGFL
C. elegans TFG1-195
Human TFGFL
Human TFG1-193
c
MW
CeTFG1-195
HsTFG1-193
250
150
100
75
50
37
25
20
15
10
=
MW
CeTFGFL
HsTFGFL
250
150
100
75
50
37
25
20
15

a

```
H. sapiens TFG  MNGQLDLSGKLIIKAQLGEDIRRIPIHN-EDITYDELVLMMQRVFRGKLLSNDEVTIKYK
C. elegans TFG  MVHSNGAITSTILKARHADVVRKTSLHHANDLTLIDLVLNVQRLLA--LPSDANFVLKYK
                *          * **      *    *   * *   ***  **      * *      ***

H. sapiens TFG  DEDGDLITIFDSSDLSFAIQCS-RILKLTLFVNGQPRPLESSQVKYLRRELIELRNKVNR
C. elegans TFG  DEEGDLVTLAEDSDLLLALHTSGATLDVTVVVDSRAR----EAVHDVQKQVEQIKLDVGK
                ** *** *    ***  *   *   *  * *   *      *               *

H. sapiens TFG  LLDSLEPPGEPGPSTNIPENDTVDGREEKSASD-----SSGKQSTQVMAASMSAFDPLKN
C. elegans TFG  LLGALSALDVAQIAEQSNTSVANLSAPKQSHHDNIVFQKSFEAAPPSPVPSEKAELPATI
                **  *                        *  *      *          *  *  *

H. sapiens TFG  QDEINKNVMSAFGLTDDQVS
C. elegans TFG  QPSVHEQFNHRPAHVEEEIP
                *
```

b

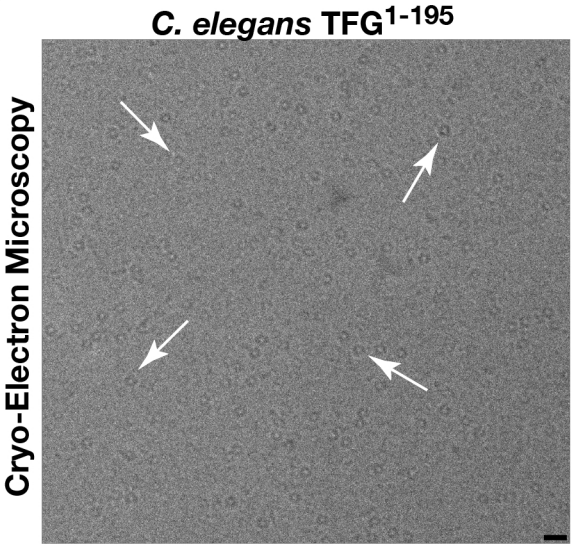

c

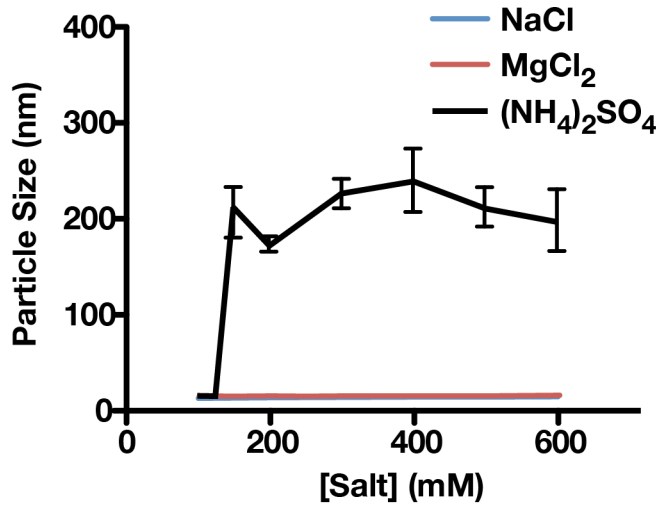

a

H. sapiens TFG

MNGQLDLSGKLIIKAQLGEDIRRIP
IHNEDITYDELVLMMQRVFRGKLLS
NDEVTIKYKDEDGDLITIFDSSDLS
FAIQCSRILKLTLFVNGQPRPLESS
QVKYLRRELIELRNKVNRLLDSLEP
PGEPGPSTNIPENDTVDGREEKSAS
DSSGKQSTQVMAASMSAFDPLKNQD
EINKNVMSAFGLTDDQVSGPPSAPA
EDRSGTPDSIASSSSAAHPPGVQPQ
QPPYTGAQTQAGQIEGQMYQQYQQQ
AGYGAQQPQAPPQQPQQYGISQYSA
YSQQTGPQQPQQFQGYGQQPTSQAP
APAFSGQPQQLPAQPPQQYQASNYP
AQTYTAQTSQPTNYTVAPASQPGMA
PSQPGAYQPRPGFTSLPGSTMTPPP
SGPNPYARNRPPFGQGYTQPGPGYR

Helix Sheet Disordered

b

C. elegans TFG

MVHSNGAITSTILKARHADVVRKTS
LHHANDLTLIDLVLNVQRLLALPSD
ANFVLKYKDEEGDLVTLAEDSDLLL
ALHTSGATLDVTVVVDSRAREAVHD
VQKQVEQIKLDVGKLLGALSALDVA
QIAEQSNTSVANLSAPKQSHHDNIV
FQKSFEAAPPSPVPSEKAELPATIQ
PSVHEQFNHRPAHVEEEIPLENHYA
PPPHQQIPDDLNTSFSSQPPPPIEQ
FGAIPPPNATIPSFPTSNAASPPVQ
EFAPPPPQQQQQQFQAPPPPMASHS
SISSTPVQQQGFAPPQQFGGPPPSG
PPSEYGGYAPPQQQQQQFGAPPPQG
APQQGFGAPPQGPPQGGPPQGSFGA
PPPQQFHAPSPQSFGGPPPPVSSAP
GNFAPPPQSGPPGAFAPPPSAFGAP
QGPGGPGGYGPPPPGGPGAPGSYGP
PQGGPGGFGPPPPGGPGAYGPPPTG
FPPVGAPPPGAAGAPGGNPFARGPS
ATGYRQSPYQQ

c

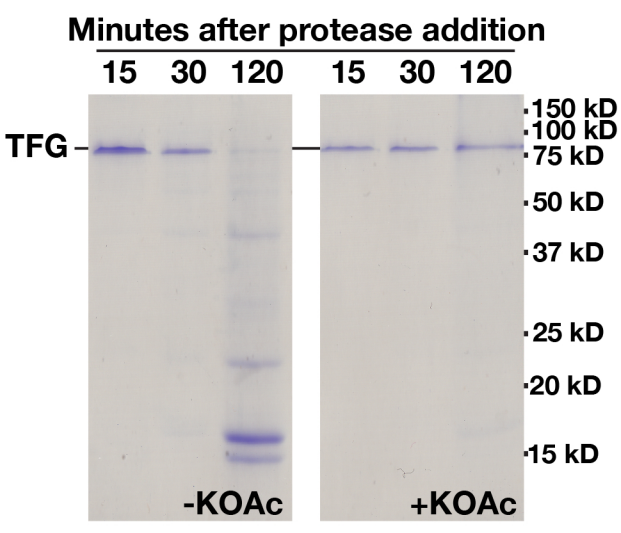

a

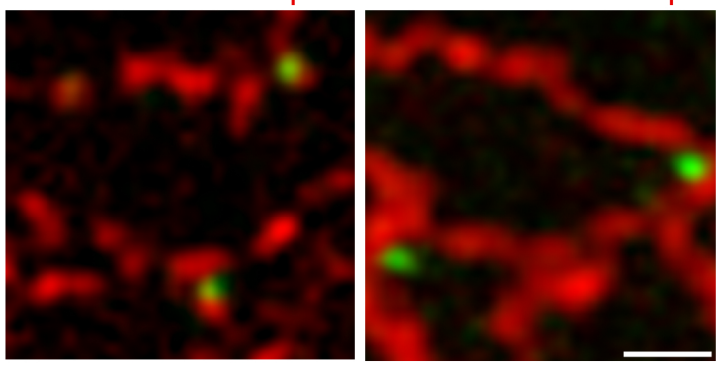
Sec16A / Sec61β
ERGIC-53 / Sec61β

b

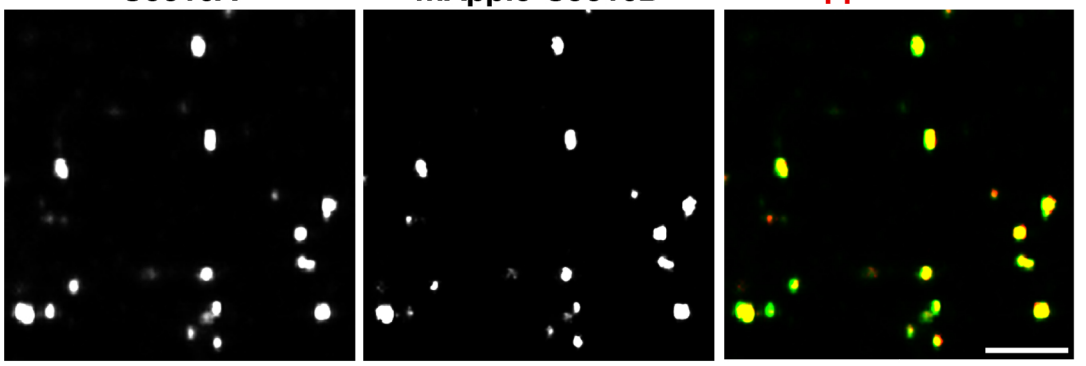
Sec16A
mApple-Sec16B
Sec16A /
mApple-Sec16B

c

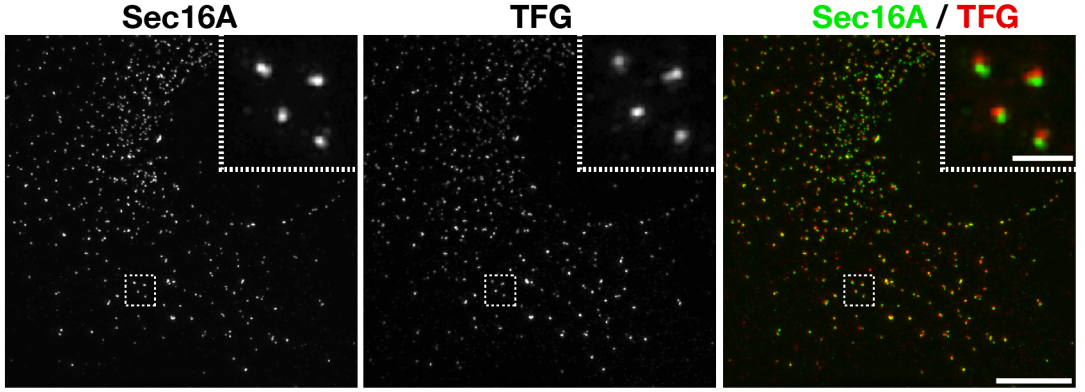
Sec16A
TFG
Sec16A / TFG

d

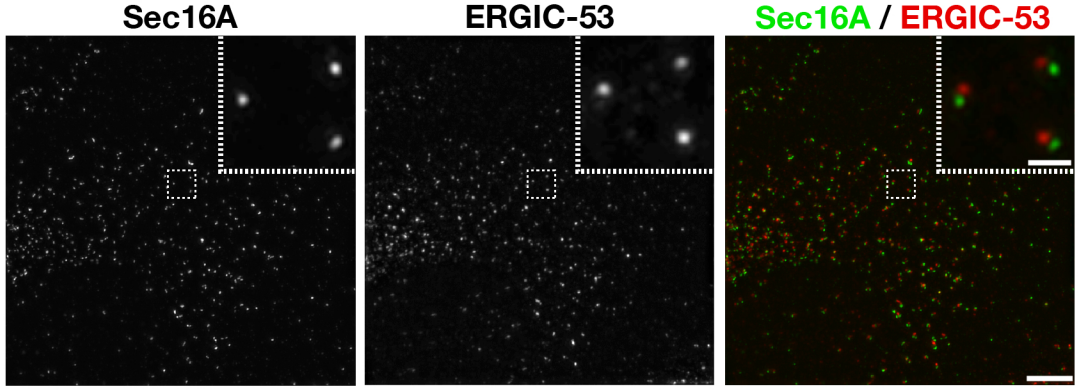
Sec16A
ERGIC-53
Sec16A / ERGIC-53

e

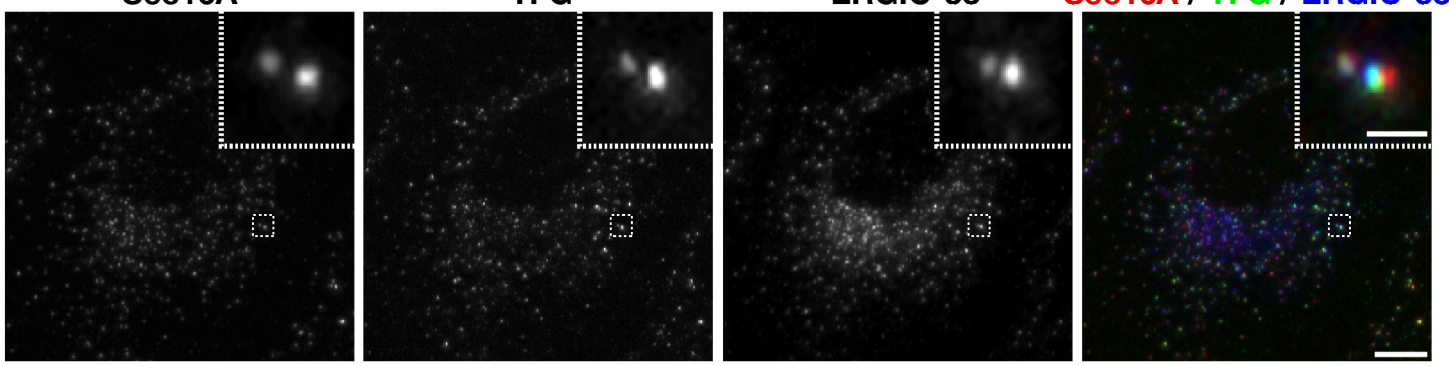
Sec16A
TFG
ERGIC-53
Sec16A / TFG / ERGIC-53

f

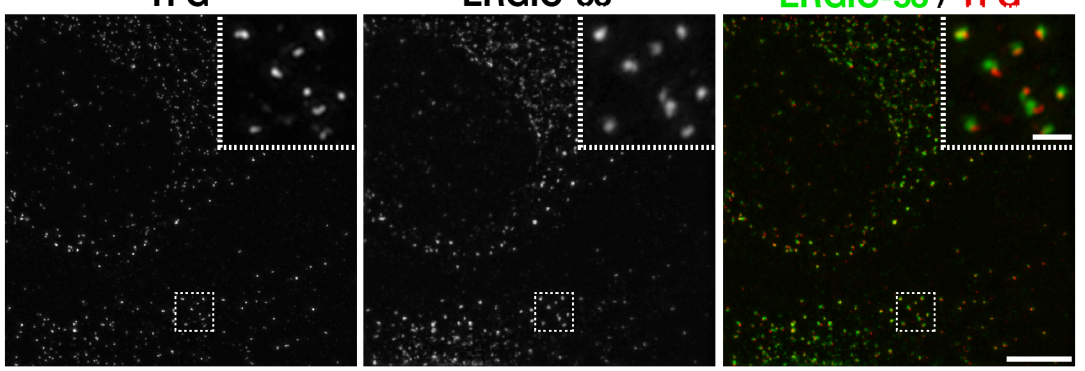
TFG
ERGIC-53
ERGIC-53 / TFG

g

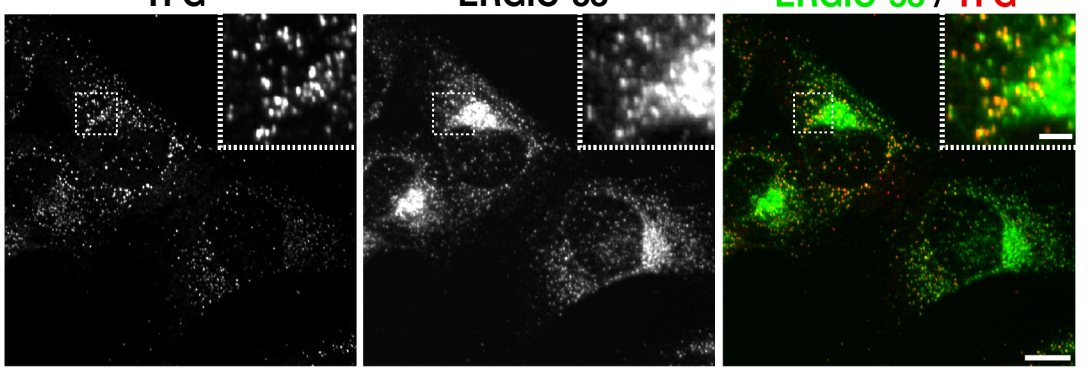
TFG
ERGIC-53
ERGIC-53 / TFG

h

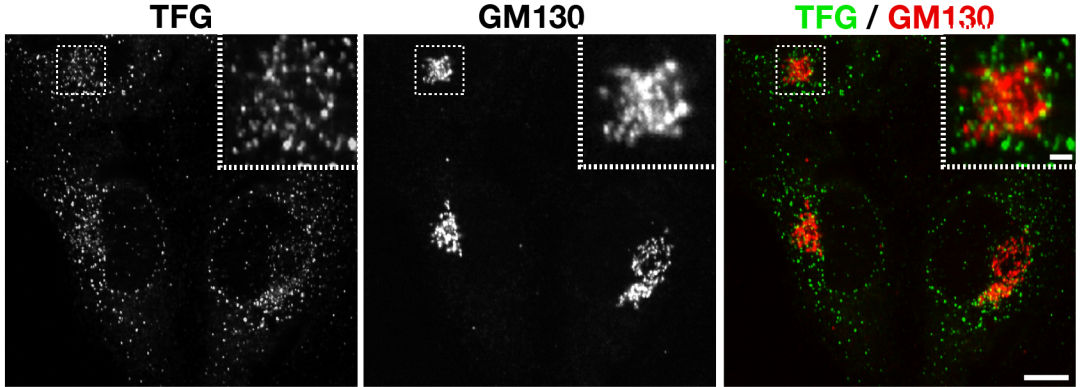
TFG
GM130
TFG / GM130

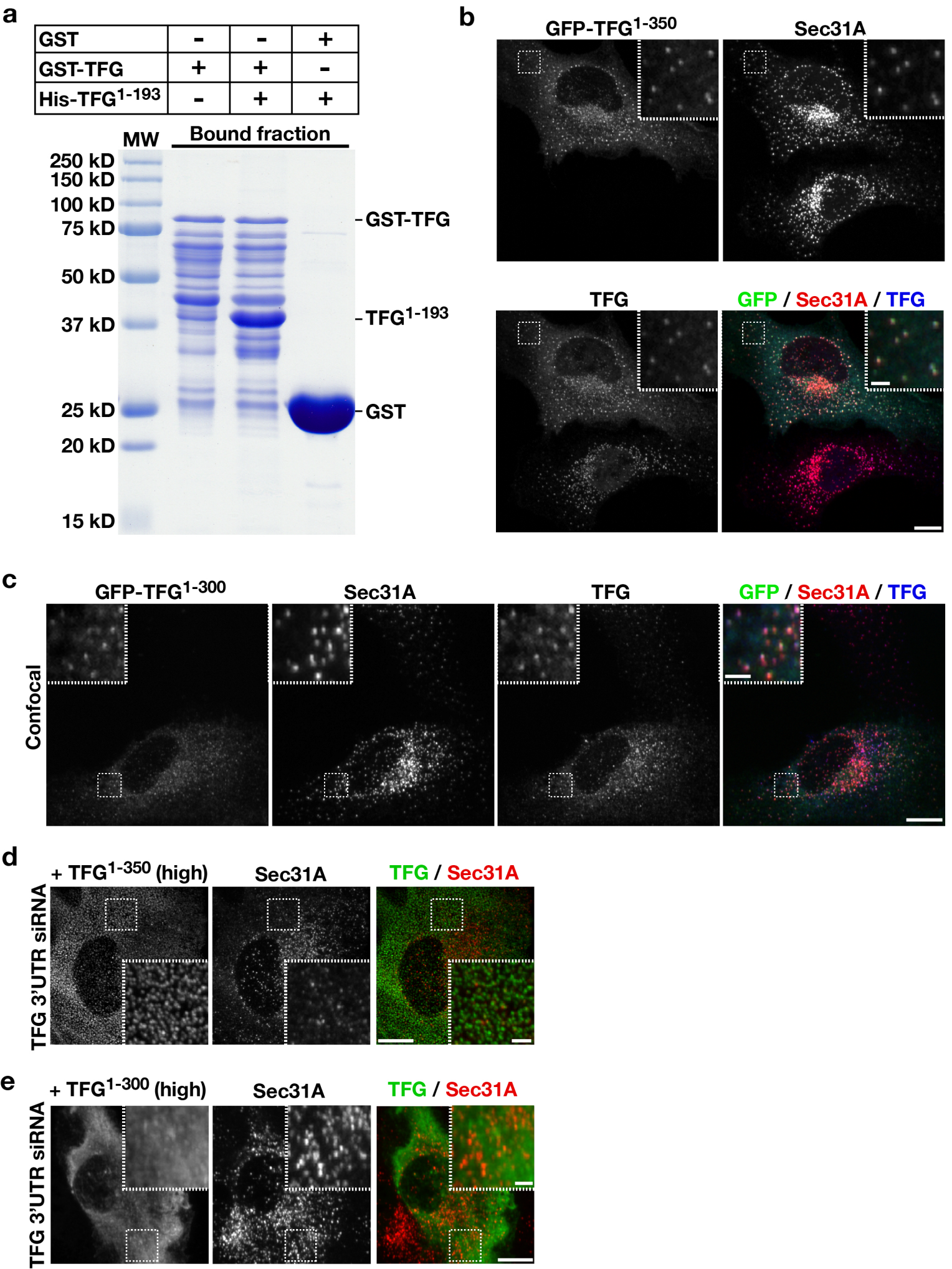
a
GST - - +
GST-TFG + + -
His-TFG1-193 - + +
MW
Bound fraction
250 kD
150 kD
100 kD
75 kD
50 kD
37 kD
25 kD
20 kD
15 kD
GST-TFG
TFG1-193
GST
b
GFP-TFG1-350
Sec31A
TFG
GFP / Sec31A / TFG
c
GFP-TFG1-300
Sec31A
TFG
GFP / Sec31A / TFG
Confocal
d
+ TFG1-350 (high)
Sec31A
TFG / Sec31A
TFG 3'UTR siRNA
e
+ TFG1-300 (high)
Sec31A
TFG / Sec31A
TFG 3'UTR siRNA

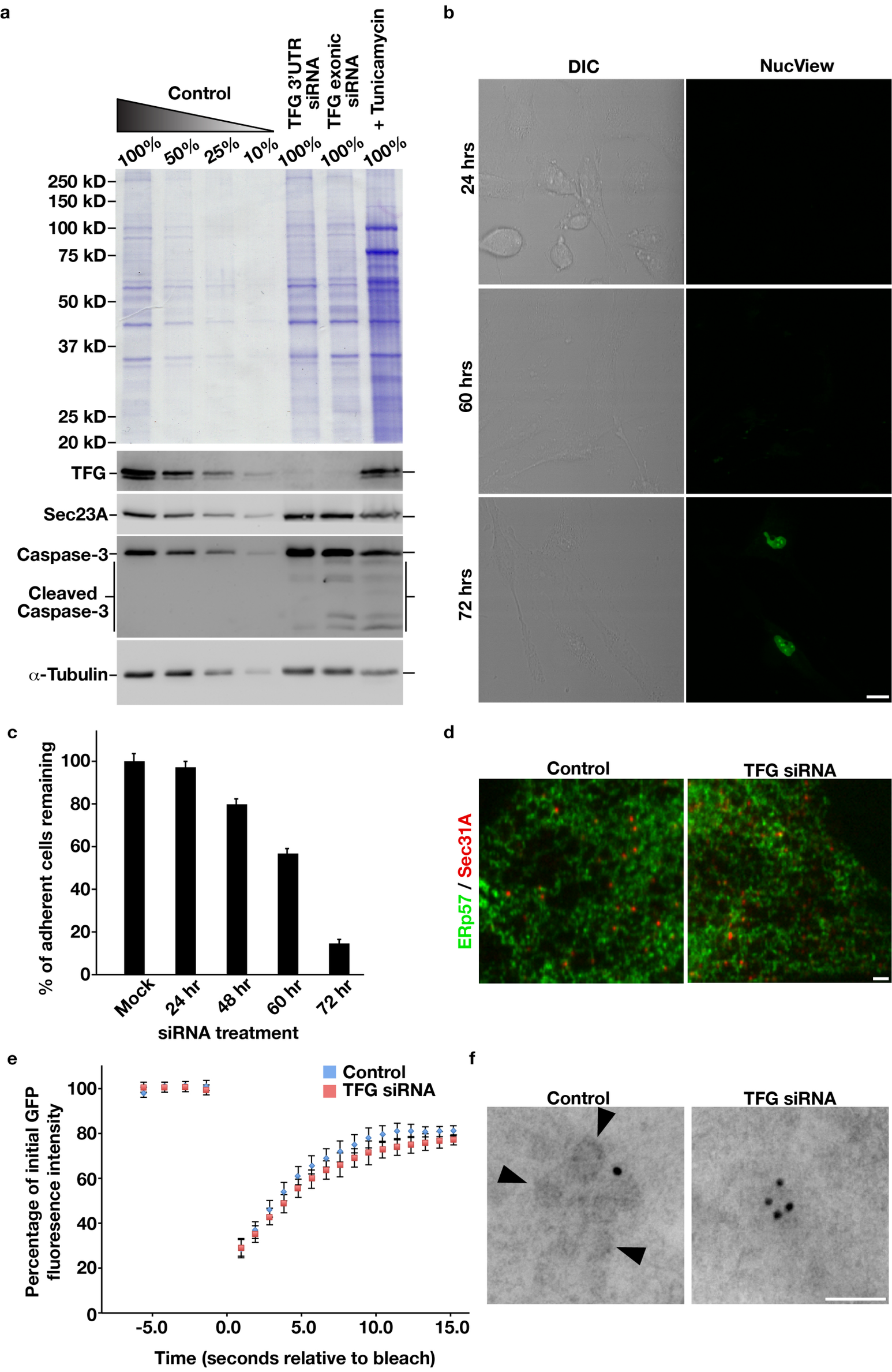
a
Control
TFG 3'UTR siRNA
TFG exonic siRNA
+ Tunicamycin
100%
50%
25%
10%
100%
100%
100%
250 kD
150 kD
100 kD
75 kD
50 kD
37 kD
25 kD
20 kD
TFG
Sec23A
Caspase-3
Cleaved Caspase-3
α-Tubulin
b
DIC
NucView
24 hrs
60 hrs
72 hrs
c
% of adherent cells remaining
100
80
60
40
20
0
Mock
24 hr
48 hr
60 hr
72 hr
siRNA treatment
d
Control
TFG siRNA
ERp57 / Sec31A
e
Control
TFG siRNA
Percentage of initial GFP fluorescence intensity
100
80
60
40
20
0
-5.0
0.0
5.0
10.0
15.0
Time (seconds relative to bleach)
f
Control
TFG siRNA

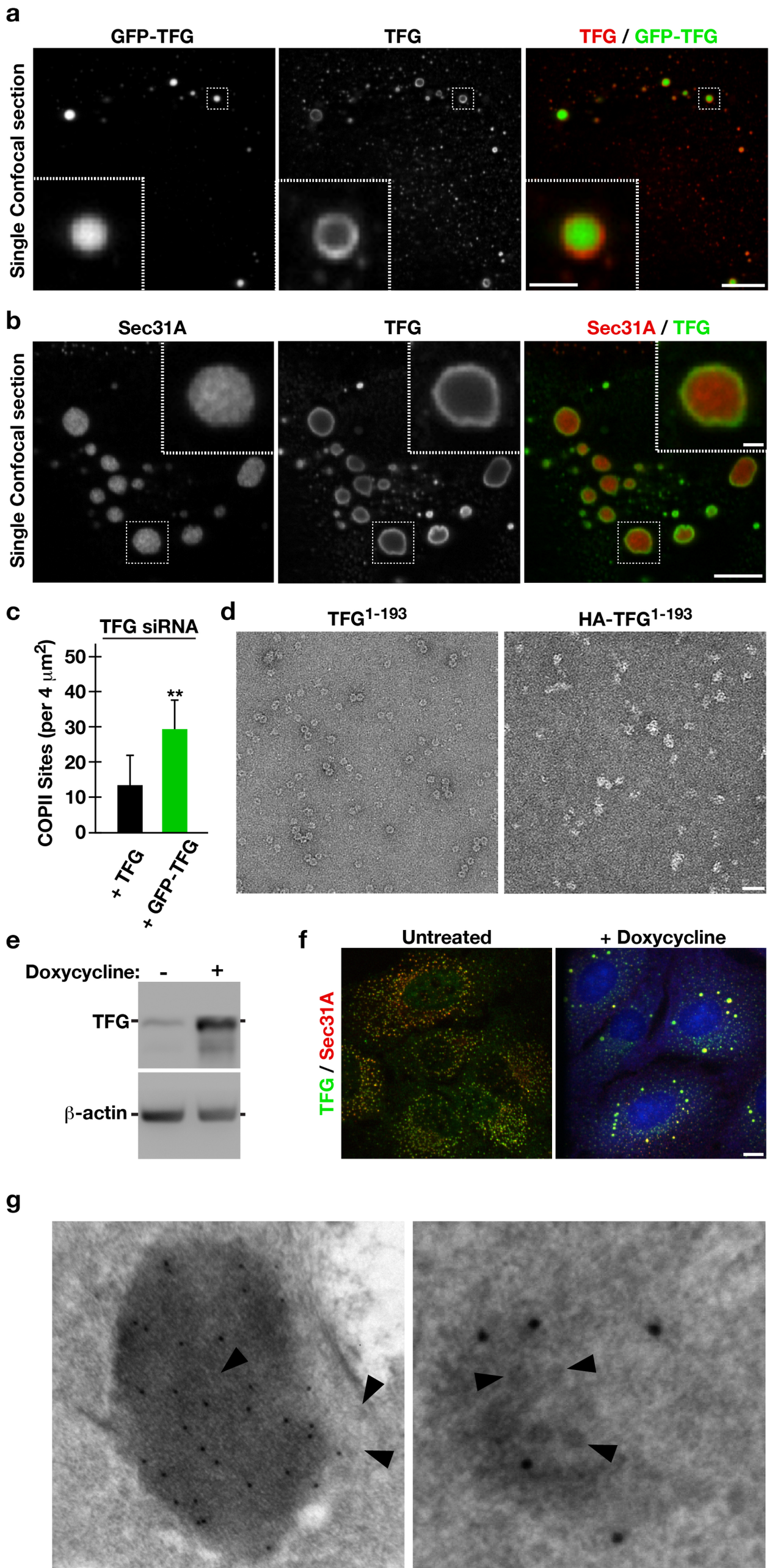
a
GFP-TFG
TFG
TFG / GFP-TFG
Single Confocal section
b
Sec31A
TFG
Sec31A / TFG
Single Confocal section
c
TFG siRNA
COPII Sites (per 4 μm2)
50
40
30
20
10
0
**
+ TFG
+ GFP-TFG
d
TFG1-193
HA-TFG1-193
e
Doxycycline: - +
TFG
β-actin
f
Untreated
+ Doxycycline
TFG / Sec31A
g

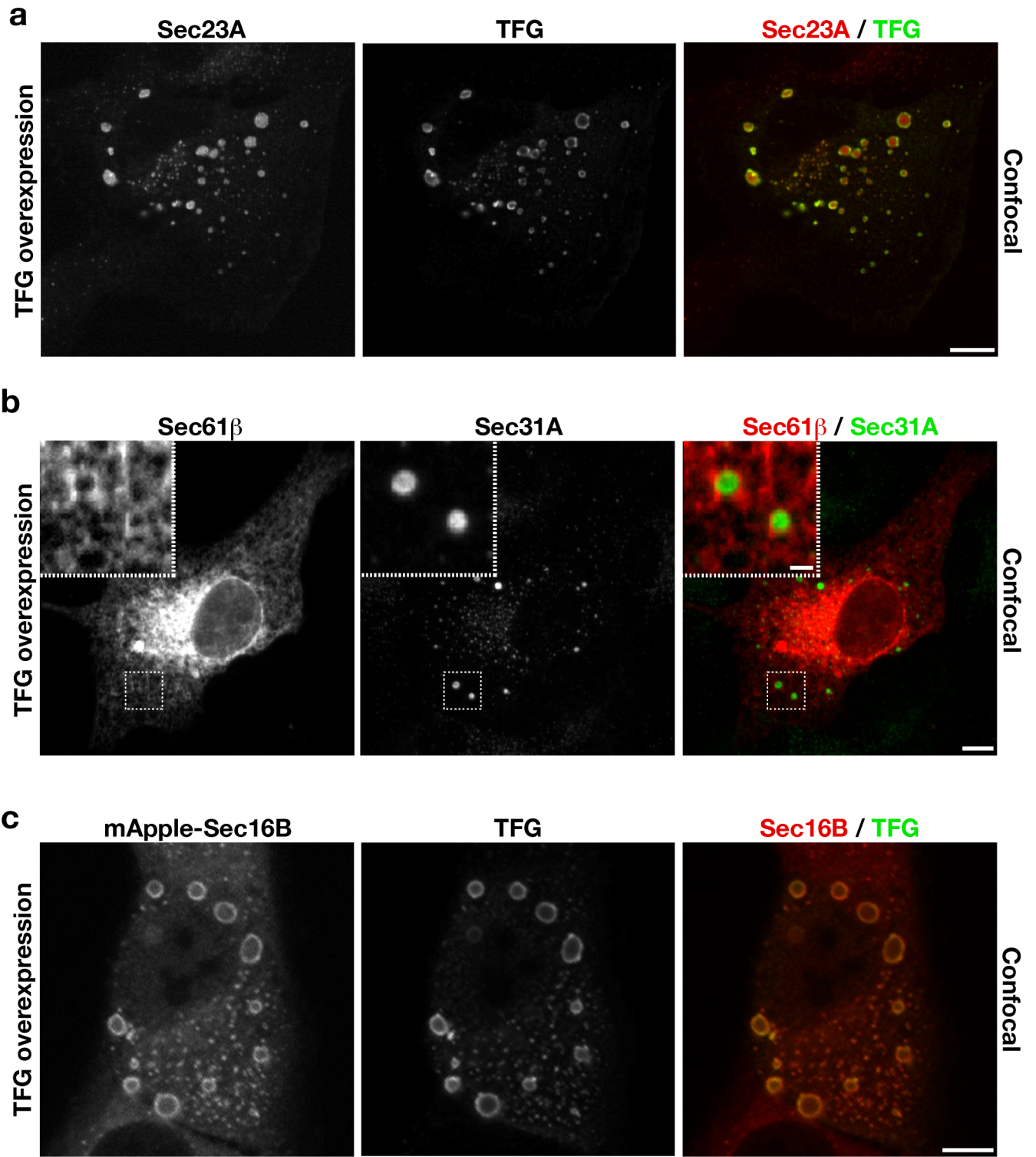
a
Sec23A
TFG
Sec23A / TFG
TFG overexpression
Confocal
b
Sec61β
Sec31A
Sec61β / Sec31A
TFG overexpression
Confocal
c
mApple-Sec16B
TFG
Sec16B / TFG
TFG overexpression
Confocal

a

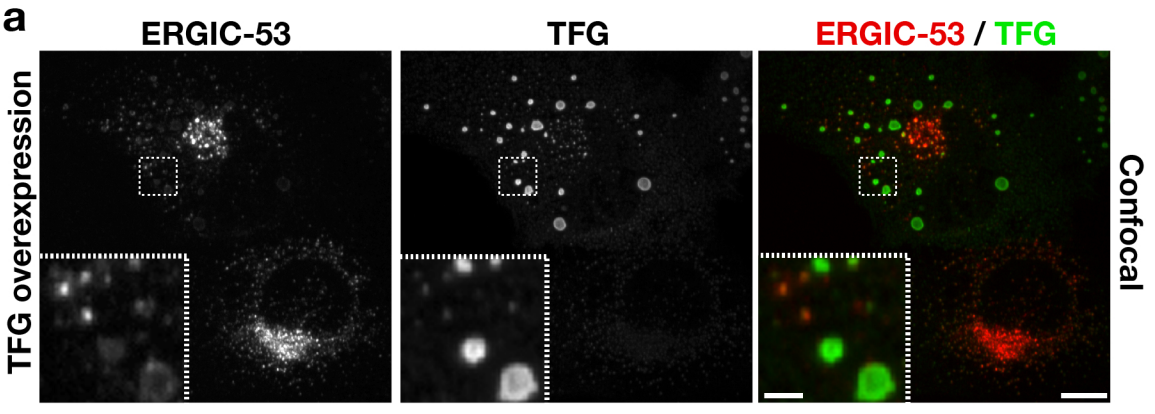
ERGIC-53
TFG
ERGIC-53 / TFG
TFG overexpression
Confocal

b

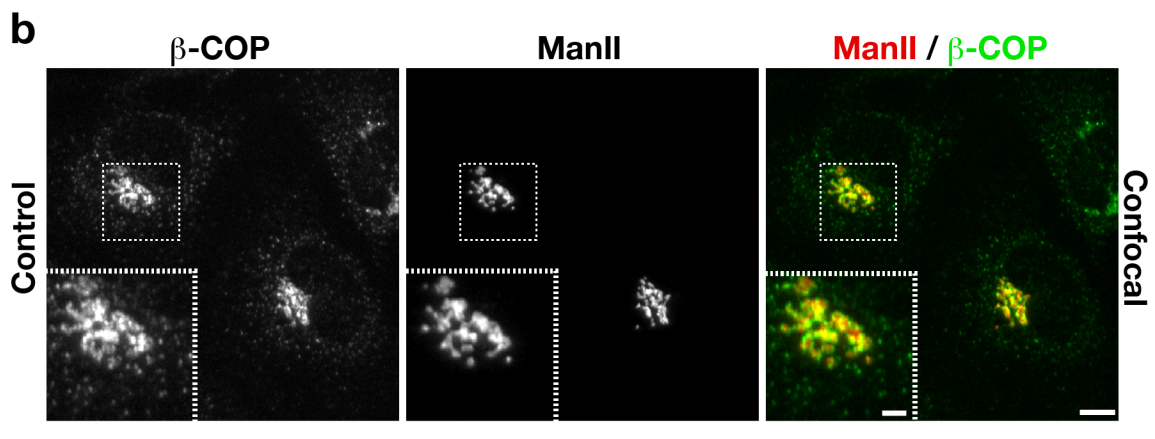
β-COP
ManII
ManII / β-COP
Control
Confocal

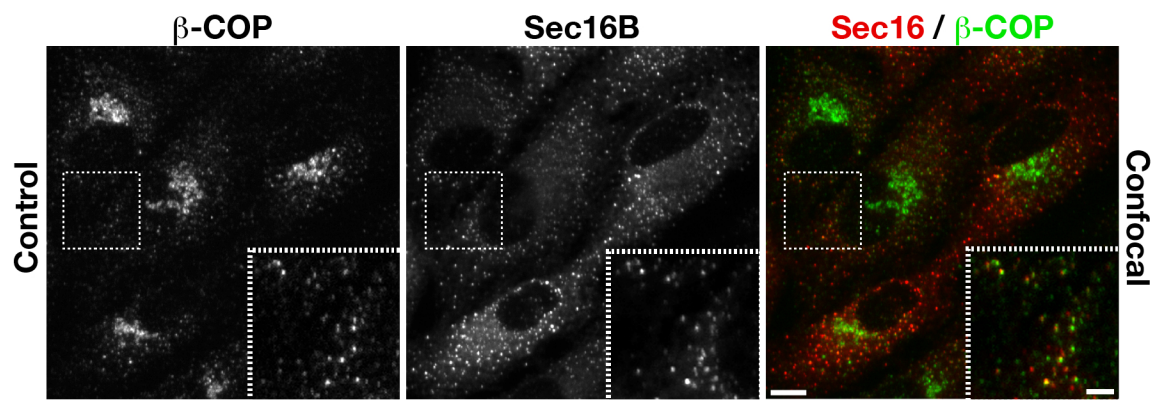
β-COP
Sec16B
Sec16 / β-COP
Control
Confocal

c

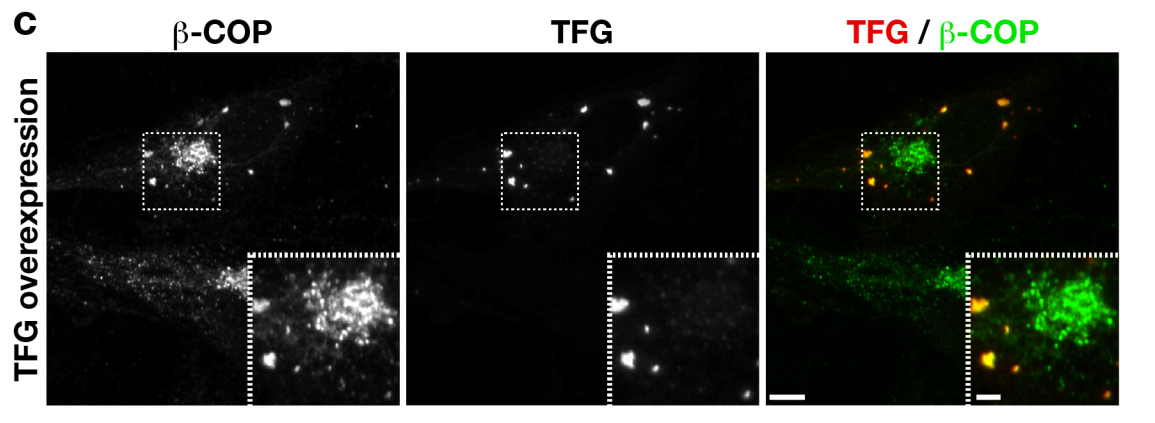
β-COP
TFG
TFG / β-COP
TFG overexpression

d

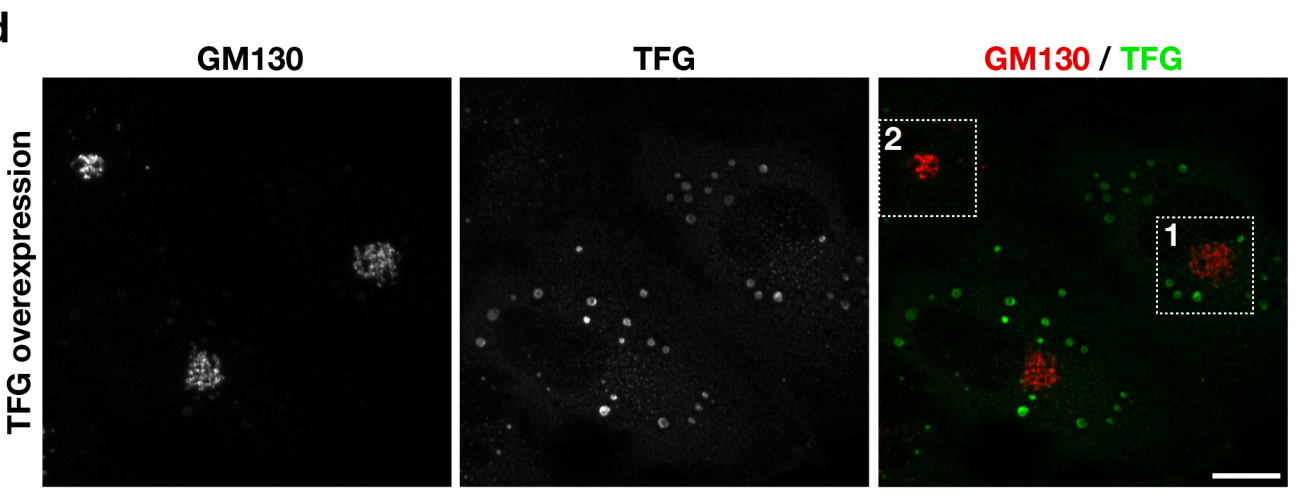
GM130
TFG
GM130 / TFG
TFG overexpression
2
1

e

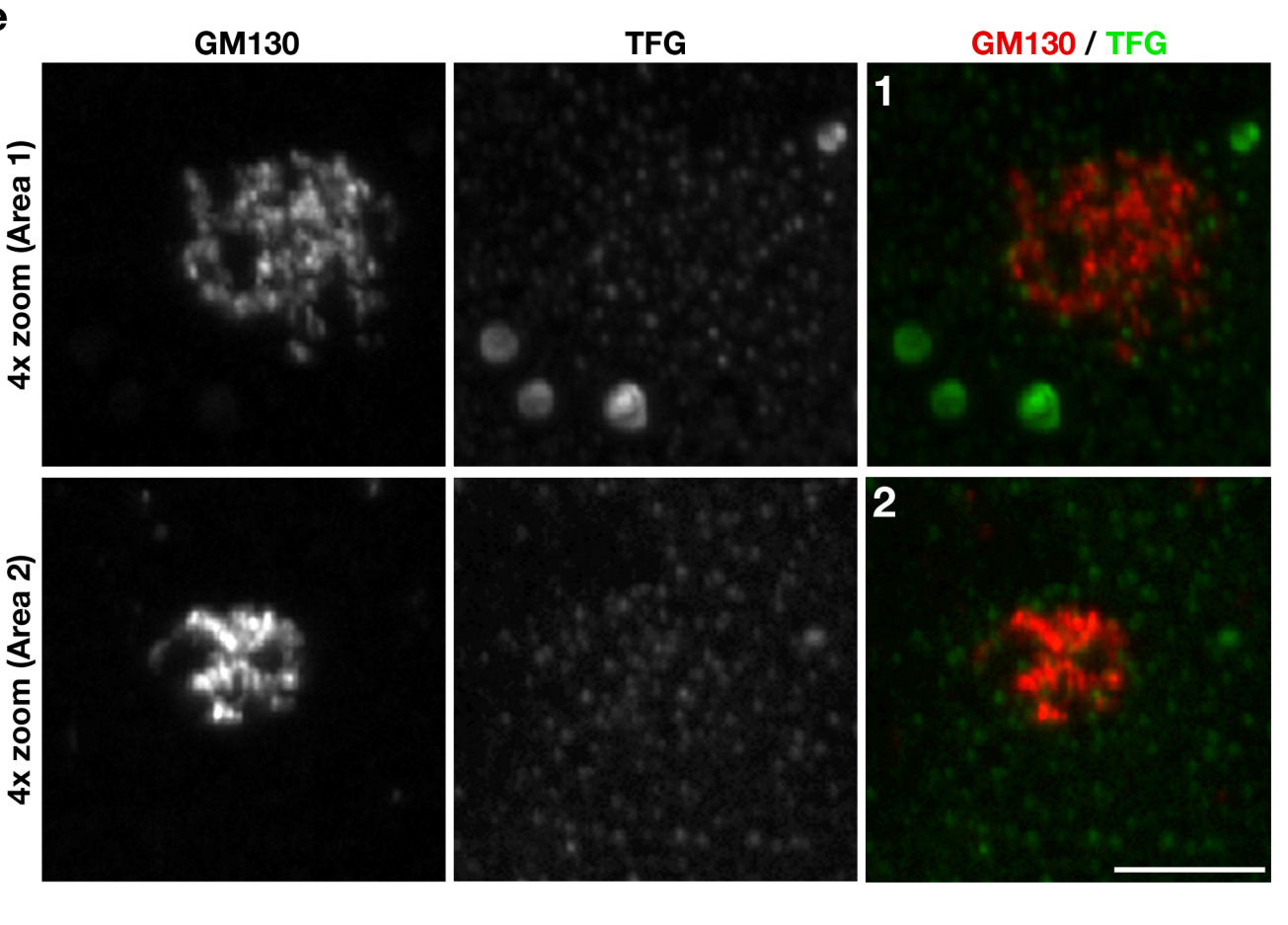
GM130
TFG
GM130 / TFG
4x zoom (Area 1)
4x zoom (Area 2)
1
2

f

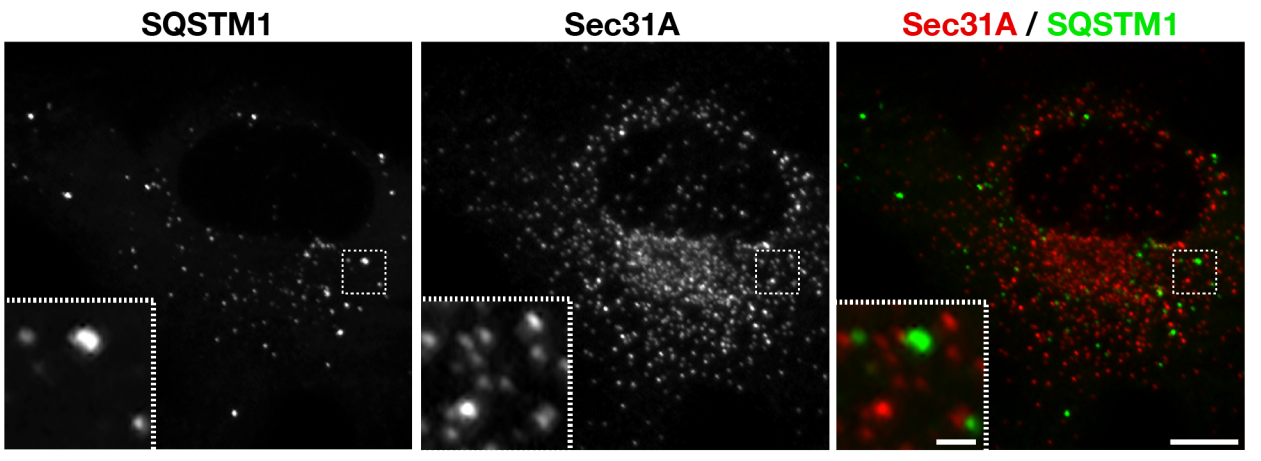
SQSTM1
Sec31A
Sec31A / SQSTM1

g

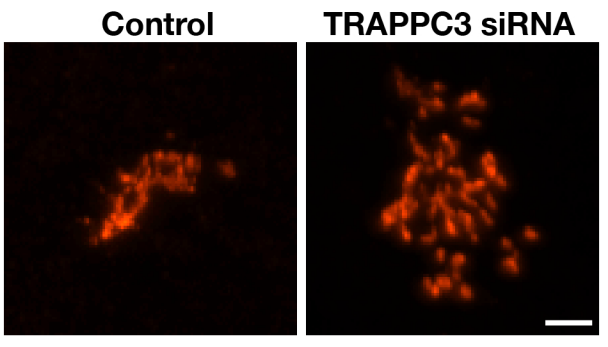
Control
TRAPPC3 siRNA
GM130

h

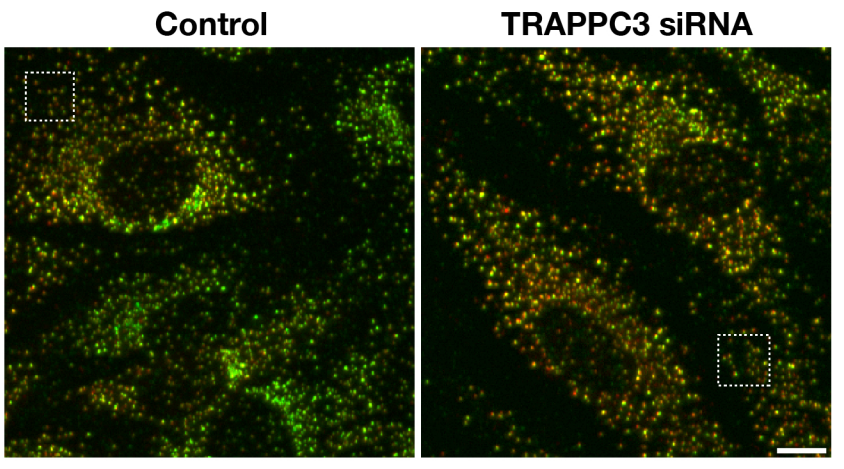
Control
TRAPPC3 siRNA
Sec16A / Sec31A

i

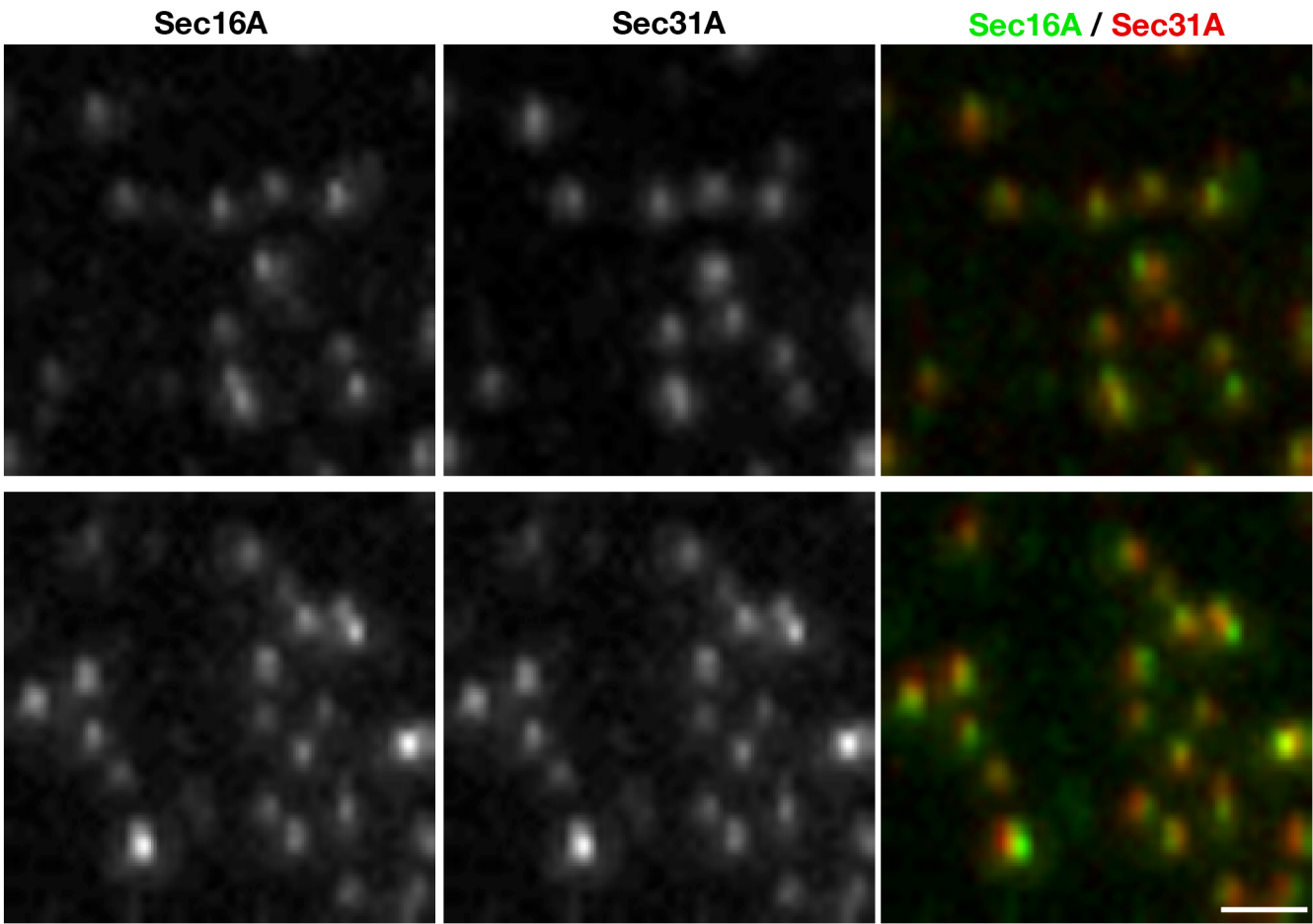
Sec16A
Sec31A
Sec16A / Sec31A
Control
TRAPPC3 siRNA

Table S1. Fourier shell correlation (FSC) resolution measurements for each human TFG^{1-193} structure determined was based on 18,102 total particle pairs.

Volume	No. Of Particles used	FSC Resolution (Å)
1	629	32.86
2	621	34.7
3	801	34.03
4	454	38.62
5	767	32.08
6	738	33.48
7	577	35.0
8	827	31.2

Table S2. Fourier shell correlation (FSC) resolution measurements for each *C. elegans* TFG^{1-195} structure determined was based on 33,720 total particle pairs.

Volume	No. of particles used	FSC Resolution (Å)
1	1478	27.58
2	1279	30.63
3	869	30.66
4	1219	31.02
5	1204	27.7
6	941	30.12
7	495	36.9
8	1139	27.93